ISSN: 2710-0588

Finite Element Analysis of Bonding Performance of Prestressed CFRP-Steel Interface

Chenghao Xu, Xiang Wang, Linchuan Li

School of Liaoning Petrochemical University, Fushun 113000, China

Abstract

In order to investigate the bonding performance of the interface between prestressed CFRP fabric and steel, a prestressed CFRP-steel single-shear specimen was modeled using ABAQUS. The nonlinear bond-slip characteristics of the interface were simulated by utilizing the cohesion unit. The impact of various factors such as the degree of pre-stressing of CFRP fabric, number of layers, pasting width, paste length, and thickness of the adhesive layer on the interface bond performance of the prestressed CFRP-steel single-shear specimens was analyzed. The simulation results indicate that the primary cause of failure for the prestressed CFRP-steel interface is cohesive damage to the adhesive layer. The presence of prestressing allows the adhesive layer of the specimen to offset part of the external force, improving the interfacial bonding performance. The load-end displacement curves of the prestressed CFRP-steel specimens display a two-phase development law. The ultimate load of the specimen is increased by the degree of prestressing of the CFRP fabric, the pasting width, and the adhesive layer thickness. As the adhesive layer thickness, adhesive width, and CFRP fabric prestressing increase, the ultimate load and ductility of the specimens also increase. However, adding more layers of CFRP fabric will only lead to a higher ultimate load and reduced ductility for the specimens. An increase in adhesive layer thickness in the 0.3~0.7 mm range results in a nonlinear improvement in interfacial stiffness. On the other hand, a linear improvement in interfacial stiffness is observed by increasing the number of layers of CFRP cloth prestressing within the range of 1~3, resulting in a 24% increase for each additional layer.

Keywords

ABAQUS; Prestressed CFRP-steel interface; Prestressing; Bond performance; Single shear specimen.

1. Introduction

One of the major areas of research in the field of structural reinforcement and repair in civil engineering is the investigation of the interfacial bonding performance between steel and carbon fiber reinforced composite fabric, or "CFRP fabric". CFRP material has been extensively utilized in the reinforcement of bridges, buildings, and other engineering structures due to the ongoing advancements in modern engineering technology. These advantages include the material's lightweight, high strength, resistance to corrosion, ease of construction, and efficient avoidance of stress concentration[1-6]. However, the reinforcement effect and long-term stability of the structure are strongly impacted by the interfacial bonding performance between CFRP and steel structures [8–10]. Consequently, a thorough analysis of it has substantial theoretical and practical implications. The shear resistance of the CFRP-bonded interface, binder, and steel-bonded interface work together to produce the bond performance of the CFRP-steel interface. The strength of the steel-bonded interface and CFRP-bonded interface is dependent on the interfacial bonding force [11]. The failure modes of CFRP-reinforced steel structures include steel-bond interface peeling, bond layer failure, CFRP-bond interface peeling,

ISSN: 2710-0588

CFRP material fracture, CFRP interlayer peeling, and steel yielding, according to a summary of numerous studies on the subject by Zhao et al. [12]. According to Teng, J. G. et al. [8], the most ideal failure mechanism for the CFRP-steel interface is interface failure that occurs in the bond layer. Yiyan Lu et al. [13] conducted double shear tests on CFRP-steel plate specimens to investigate the effects of CFRP adhesive length, adhesive width, and the number of adhesive layers on bond performance and failure mode at the interface. The results showed that the number of adhesive layers in CFRP is associated with its finite adhesive length, which increases progressively with the number of layers.

Under the impact of tensile force, CFRP experiences significant tensile deformation due to its large fracture strain. The strong strength performance of CFRP is often underutilized in reinforcing other structures [14–15]. Several academics have proposed the prestressed composite reinforcement approach as a solution to this issue [16–17]. To maximize the high-strength performance of CFRP and enhance the stiffness of the reinforced components, this procedure involves prestressing the CFRP fabric with steel plates. Nevertheless, the complex bonding process at the interface between prestressed CFRP fabric and steel is determined by a number of variables, including the loading mode, interface treatment, and material characteristics. The bonding performance between prestressed CFRP and steel structures has been the subject of comparatively few investigations, and many issues are still unresolved. Structural interface peeling damage frequently occurs a few to several millimeters below the surface in experimental studies [18]. Directly measuring interface behavior is challenging, and calculating the CFRP fabric strain distribution is a common method used to determine interfacial shear stress and slip, which can introduce significant bias. Consequently, conducting a comprehensive investigation of the prestressed CFRP-steel interface through physical experiments that measure the CFRP fabric strain is difficult [19]. On the other hand, the bond performance and stress distribution law of the prestressed CFRP-steel interface can be effectively studied using numerical simulation methods [20]. Therefore, this study utilizes cohesive units to simulate the nonlinear bond-slip properties of the interface using ABAQUS finite element software. The aim of the research is to investigate the bond performance of the interface between prestressed CFRP fabric and steel, as well as the factors that affect it under various prestressing levels, number of layers, adhesive layer thickness, bond length, and bond width.

2. Model Specimen Design

Table 1. Finite element model parameters

Test piece	Degree of prestressing of CFRP fabric	CFRP cloth paste width	Thickness of bonding layer	Layers of CFRP fabric	CFRP Cloth Paste Length
BZ-1	10%	100mm	0.5mm	1	250mm
A-1	5%	100mm	0.5mm	1	250mm
A-2	15%	100mm	0.5mm	1	250mm
B-1	10%	80mm	0.5mm	1	250mm
B-2	10%	120mm	0.5mm	1	250mm
C-1	10%	100mm	0.3mm	1	250mm
C-2	10%	100mm	0.7mm	1	250mm
D-1	10%	100mm	0.5mm	2	250mm
D-2	10%	100mm	0.5mm	3	250mm
E-1	10%	100mm	0.5mm	1	210mm
E-2	10%	100mm	0.5mm	1	230mm

ISSN: 2710-0588

A length of prestressed CFRP fabric was used to bond two steel plates together to create a "whole" in each of the five sets of specimens that were designed; the composition of these sets is illustrated in Fig. 1. To accurately replicate the stress performance of the CFRP-steel interface and analyze the bonding performance of the interface, this specimen ensures that the CFRP fabric is solely under tensile stress and that the adhesive layer is only subjected to shear stress [21–24]. The steel plate measures 200 x 250 mm and is constructed from Q235 grade steel. The CFRP utilizes Class I carbon fiber cloth, with 0.167 mm in thickness, 3500 MPa tensile strength, and 230 GPa modulus of elasticity. Standard specimen BZ-1 is categorized with other specimens based on specific criteria, as outlined in Table 1.

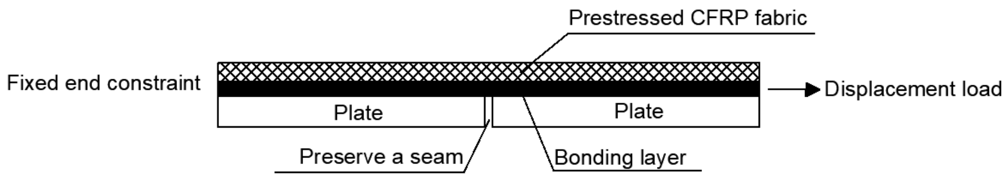

Figure 1. Schematic diagram of single shear specimen

3. Finite Element Model

3.1. Modeling assumptions

These fundamental assumptions are established for the modeling process to ensure that the CFRP-adhesive layer-steel plate finite element model is practical for engineering applications.

(1) The steel plate is isotropic, the CFRP fabric is anisotropic, and the test material is homogeneous and continuous.

(2) During the loading process, the prestressed CFRP fabric maintains linear elasticity at all times.

(3) No stripping damage is taken into consideration, and there is no relative sliding between the layers of prestressed CFRP fabric.

(4) Neither the interface between the steel plate and the adhesive layer nor the interface between the prestressed CFRP fabric and the adhesive layer exhibits any relative sliding.

(5) Ignoring the geometric flaws in the material, as well as any potential stress concentration and residual stress that may arise during the specimen's construction.

3.2. Material principal model

In this paper, the eigenstructural relationship of the steel plate is established as a bifold ideal elastic-plastic eigenstructural model, as illustrated in Fig. 2. The analytical expression is presented below:

$$\begin{cases} E_{\varepsilon}, & \varepsilon \le \varepsilon_{\gamma} \\ f_y + E_1(\varepsilon - \varepsilon_y), & \varepsilon > \varepsilon_y \end{cases} \tag{1}$$

Where f_y、ε_y for the steel yield corresponding to the strength and strain values, f_u、ε_u for the ultimate strength and ultimate strain of the steel.

ISSN: 2710-0588

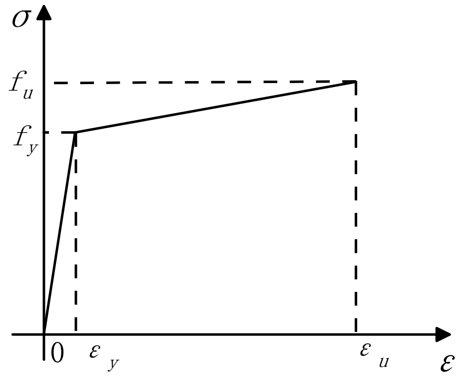

Figure 2. Stress-strain schematic of steel

The CFRP fabric principal structure relationship is shown in Fig. 3.

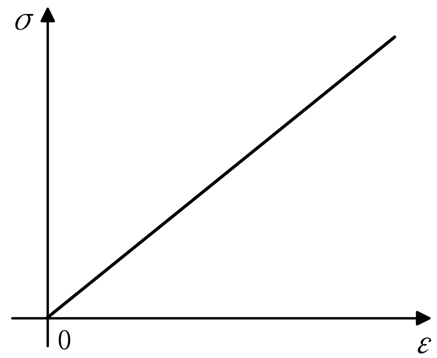

Figure 3. Stress-strain schematic of CFRP fabric

The study establishes the adhesive layer to mimic the bond slip of the interface using the traction-separation criterion cohesion unit model. To simulate bonding characteristics, the adhesion model of the adhesive layer in the finite element model must incorporate the traction-separation criterion. The stiffness and nominal stresses of the normal direction, as well as the two tangential directions combined, are input as the material parameters, and the relationship must satisfy the following:

$$\begin{bmatrix} t_{\mathrm{n}} \\ t_{\mathrm{s}} \\ t_{\mathrm{t}} \end{bmatrix} = \begin{bmatrix} K_{\mathrm{m}} & 0 & 0 \\ 0 & K_{\mathrm{ss}} & 0 \\ 0 & 0 & K_{\mathrm{tt}} \end{bmatrix} \begin{bmatrix} \varepsilon_{\mathrm{n}} \\ \varepsilon_{\mathrm{s}} \\ \varepsilon_{\mathrm{t}} \end{bmatrix} \tag{2}$$

Where, t_n, t_s and t_t are the nominal stresses in normal and two tangential directions, K_{nn}, K_{ss} and K_{tt} are the stiffnesses in three directions, ε_n, ε_s and ε_t are the nominal strains in three directions.

ISSN: 2710-0588

In this paper, the modified bond-slip calculation model by Wu Zuodong and Yang Yi et al. [25] is utilized. This model integrates various experimental data and makes necessary adjustments to the Xia model [26]. When compared to the original bond-slip parameter models, it demonstrates improved fitting and predictive capabilities for the bond performance at the interface between steel and CFRP reinforcement.

As shown in Fig. 4. Where τ_{max}, $\delta_{initial}$, δ_{fail} denote the stress at initial damage as well as the displacement, and the displacement at complete damage, respectively. The maximum nominal stress criterion is used for the damage criterion, and the damage basis is:

$$\mathrm{Max}\left\{\frac{t_n}{t_n^0},\frac{t_s}{t_s^0},\frac{t_t}{t_t^0}\right\}=1 \tag{3}$$

where t_n^0, t_s^0 and t_t^0 represent the maximum nominal stresses for pure Type I, pure Type II and pure Type III damage, respectively.

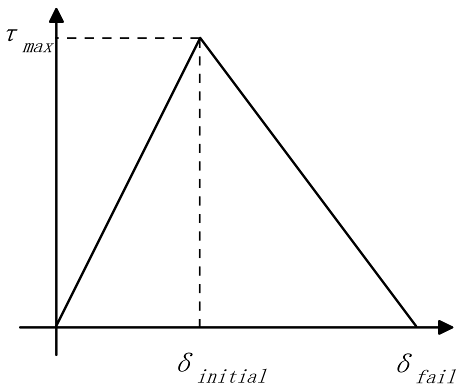

Figure 4. Bilinear ontological model of the colloid

The section headings are in boldface capital and lowercase letters. Second level headings are typed as part of the succeeding paragraph (like the subsection heading of this paragraph). All manuscripts must be in English, also the table and figure texts, otherwise we cannot publish your paper. Please keep a second copy of your manuscript in your office. When receiving the paper, we assume that the corresponding authors grant us the copyright to use the paper for the book or journal in question. When receiving the paper, we assume that the corresponding authors grant us the copyright to use the paper for the book or journal in question. When receiving the paper, we assume that the corresponding authors grant us the copyright to use.

3.3. Establishment of finite element model

Fig. 5 shows the prestressed CFRP-steel single shear specimen model established by the separated modeling approach using the finite element software ABAQUS based on the designed components and dimensions. For the prestressed CFRP fabric and the steel plate, the eight-node hexahedral cell C3D8R is chosen; for the bonding layer, the eight-node three-dimensional bonding cell COH3D8 is selected. The mesh for the prestressed CFRP fabric cell is divided into 2.5 mm, and the bonding layer cell's mesh is divided into 1 mm to balance time cost and computational accuracy. Fig. 6 displays the mesh cell division of the single-shear specimen model.

ISSN: 2710-0588

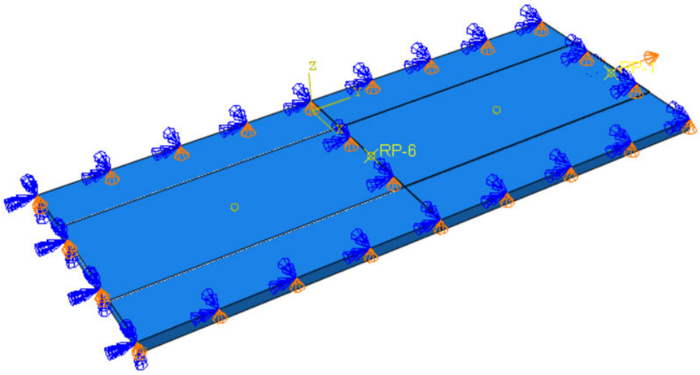

Figure 5. Model of prestressed CFRP-steel single shear specimen

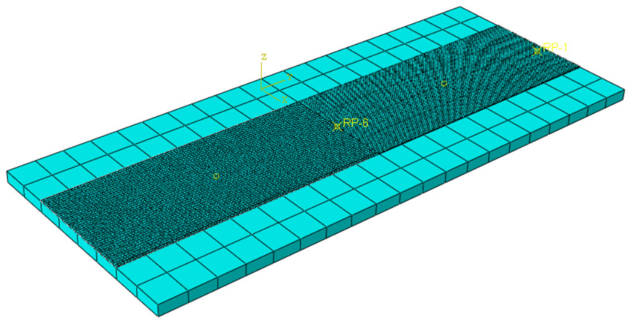

Figure 6. Single shear specimen model with grid cell division

The prestressing CFRP fabric, bonding layer, and steel plate are connected using the binding (Tie) method. The left steel plate in the model serves as the test plate and is fully fixed. The right steel plate acts as the loaded plate, with a reference point positioned at the plate's center-right and a displacement load applied. To prevent misalignment issues like the curling of the prestressed CFRP fabric during loading, it is specified that only horizontal displacement is allowed for both steel plates. The model applies prestressing force to the CFRP fabric by using the cooling approach [25]. In other words, the CFRP fabric experiences a decrease in temperature due to the preset temperature field in the ABAQUS software, resulting in a change in stress. The following formula is used to compute the temperature [26]:

$$\Delta T = \frac{\sigma}{\alpha E} \tag{4}$$

4. Model Validation

In order to verify the accuracy of this model, the specimen used in the study of CFRP-steel plate interface bonding performance based on a double shear experiment by Yang Yi et al.[21] is selected for modeling in this paper, and the results are compared to validate the model.

Table 2 presents the simulated values obtained from the finite element analysis, along with the ultimate load and ultimate displacement data from the physical specimen test. Figure 7 illustrates the load-loading end displacement curves of both the finite element simulation and the actual test specimen. A fundamental consistency is observed between the curves depicted in Figure 7 and the data in Table 2. While there are slight variations between the simulated and actual numbers, they fall within a reasonable range.

ISSN: 2710-0588

To sum up, this paper's finite element model can be used to simulate the bond performance of the prestressed CFRP-steel interface because it is rational and accurate.

Table 2. Validation of the model

Test piece	Ultimate load (kN)	Limit displacement (mm)
Simulation	24.703	1.119
Experimental	25.224	1.154
Simulation/Testing	0.979	0.97

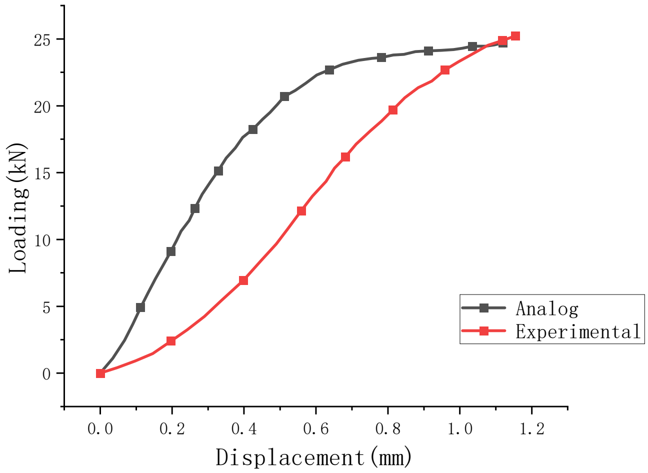

Figure 7. Comparison of load-loaded end displacement curves

5. Analysis of Results

5.1. Damage characteristics and damage mode

Through visual analysis using finite element software ABAQUS, it was observed that as the load increased, the stress on the prestressed CFRP fabric in the specimen gradually rose, leading to gradual damage in the adhesive layer until its failure. Closer to the center of the span, the damage rate was higher, and the damage was more pronounced in both layers. All five groups of specimens experienced peeling and damage, but the prestressed CFRP fabric did not reach its ultimate tensile strength. Figure 8 illustrates the damage process of the adhesive layer in specimen BZ-1, while Figure 9 displays the stress distribution in specimen BZ-1 at the point of damage.

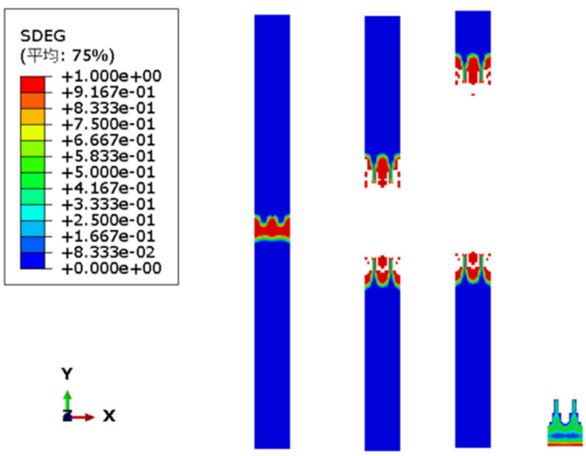

Figure 8. Damage cloud of BZ-1 adhesive layer loading process

ISSN: 2710-0588

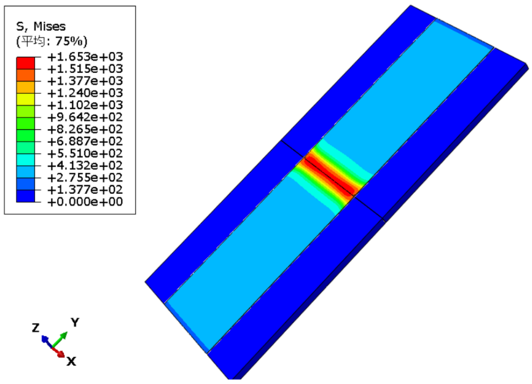

Figure 9. Stress View of Specimen BZ-1

5.2. Ultimate load

The test results for the ultimate load of each specimen are listed in Table 3.

Table 3. Main test results of each specimen

Specimen group number	*Specimen number*	*Ultimate load (kN)*	*Failure mode*
Standard part	*BZ-1*	*15.165*	*Failure of the adhesive layer*
Prestressing degree group	*A-1*	*14.002*	*Failure of the adhesive layer*
	A-2	*15.85*	*Failure of the adhesive layer*
Pasting width group	*B-1*	*7.747*	*Failure of the adhesive layer*
	B-2	*24.546*	*Failure of the adhesive layer*
Adhesive layer thickness group	*C-1*	*14.545*	*Failure of the adhesive layer*
	C-2	*16.006*	*Failure of the adhesive layer*
Array of CFRP fabric layers	*D-1*	*20.245*	*Failure of the adhesive layer*
	D-2	*23.197*	*Failure of the adhesive layer*
Bonding length group	*E-1*	*15.012*	*Failure of the adhesive layer*
	E-2	*15.165*	*Failure of the adhesive layer*

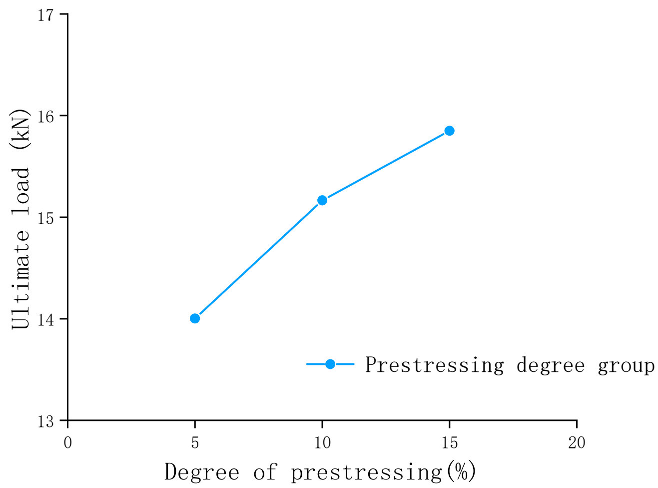

Figure 10. Effect of prestressing degree on ultimate load

ISSN: 2710-0588

The relationship between the degree of prestressing of CFRP cloth and ultimate load is illustrated in Fig. 10. As depicted in the figure, the ultimate load of the specimen demonstrates a linear increase with the rise in the degree of prestressing of the CFRP fabric. This is attributed to the transfer of prestressing to the adhesive layer through the CFRP fabric during the prestressing application process, resulting in an inward retraction force. When the specimen is loaded, the steel plate displaces to push the adhesive layer, generating an outward expansion force. Figure 11 displays the mechanical analysis model diagram of the prestressed CFRP-steel single shear specimen. Due to the thinness of the adhesive layer, the two forces are considered to counteract each other at the same level and in opposite directions within the adhesive layer, enabling the adhesive layer to withstand more shear stresses. Consequently, the application of prestressing enhances the stressing properties of the interface. Increasing the degree of prestressing of the CFRP fabric can boost the ultimate load capacity of the specimen. It is estimated that each 5% increase in the degree of prestressing raises the ultimate load of the specimen by approximately 1kN.

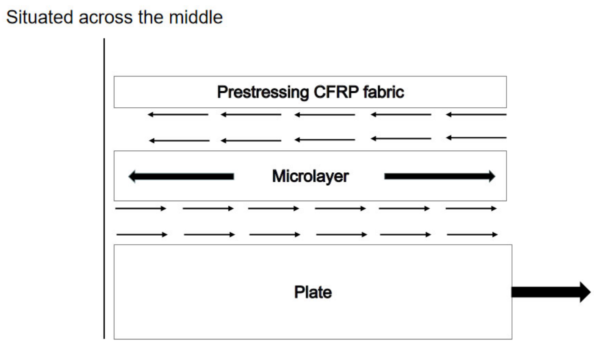

Figure 11. Mechanical analysis model diagram of prestressed CFRP-steel single shear specimen

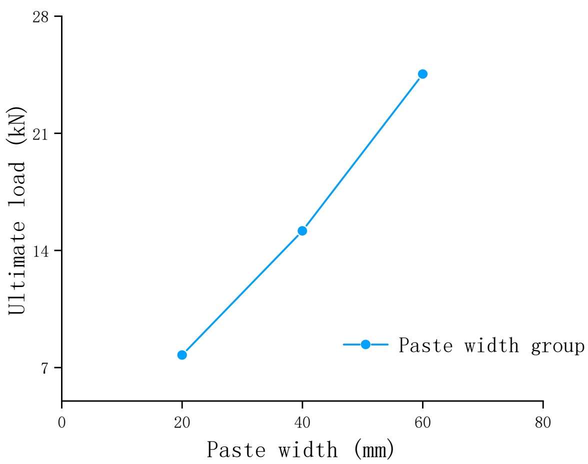

Figure 12. Effect of bond width on ultimate load

Fig. 2.7 illustrates how the bond width of the prestressed CFRP fabric affects the ultimate load. The figure shows that as the bond width of the CFRP fabric increases, the specimen's ultimate load also increases linearly. In the range of widths from 20 to 60 mm, every 20 mm increase in bond width results in an approximate 8 kN increase in the ultimate load. This is because, in

ISSN: 2710-0588

tension, the interface stress is uniform along the width of the prestressed CFRP fabric. Under the same load, increasing the bond width of the prestressed CFRP fabric reduces the shear stress at the bond interface, enhances the interface stress performance, and shifts the damage focus of the specimen mainly to the adhesive layer. Consequently, with the same adhesive layer, the ultimate load of the specimen increases linearly with the increase in bond width. Since the adhesive layer is where most of the specimen damage occurs, extending the bond width of the prestressed CFRP fabric can improve the specimen's final bearing capacity while meeting the adhesive layer's requirements.

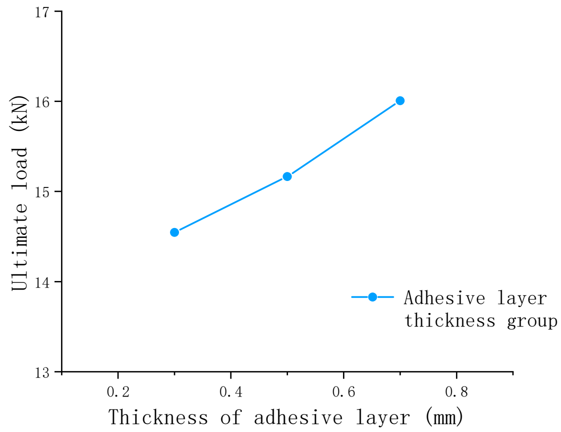

Figure 13. Effect of adhesive layer thickness on ultimate loads

Figure 13 illustrates how the thickness of the adhesive layer affects the maximum load capacity of the specimen. The figure shows that the ultimate load of the specimen increases as the adhesive layer thickness ranges from 0.3 to 0.7 mm. If the adhesive layer is too thin, it may not provide sufficient bond strength in practical CFRP reinforced steel applications. This is due to stress concentration at the bond interface, which reduces the ultimate load because a thin adhesive layer may not completely fill the small gaps between CFRP and steel. On the other hand, thick layers can result in shear failure of the adhesive layer under stress, particularly at the ultimate load. A thicker adhesive layer may be more prone to shear failure or extrusion within the adhesive layer during loading, thereby decreasing the ultimate load. According to this simulation, an adhesive layer thickness of 0.7 mm is superior to 0.3 mm and 0.5 mm, but further experiments are necessary to confirm if 0.7 mm is the optimal thickness.

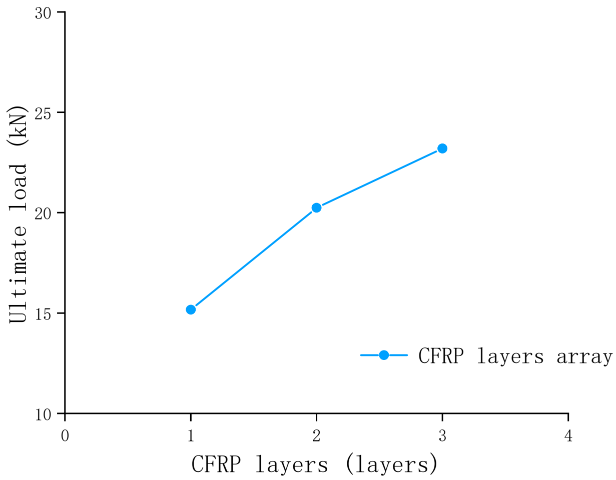

Figure 14. Effect of the number of layers of CFRP fabric on ultimate loads

ISSN: 2710-0588

The relationship between the number of layers of CFRP fabric and the ultimate load capacity of the specimens is depicted in Fig. 14. It is evident from comparing the specimens of the prestressed CFRP fabric layer groups in the table that increasing the number of bonded layers of CFRP fabric is equivalent to improving the overall tensile stiffness of CFRP fabric. The graphic illustrates how the ultimate load rises with the number of layers while the prestressed CFRP bond length remains constant. The ultimate load increases by 33.5% and 52.96%, respectively, when one layer is raised to two or three layers; the average increase for a single layer is roughly 25%.

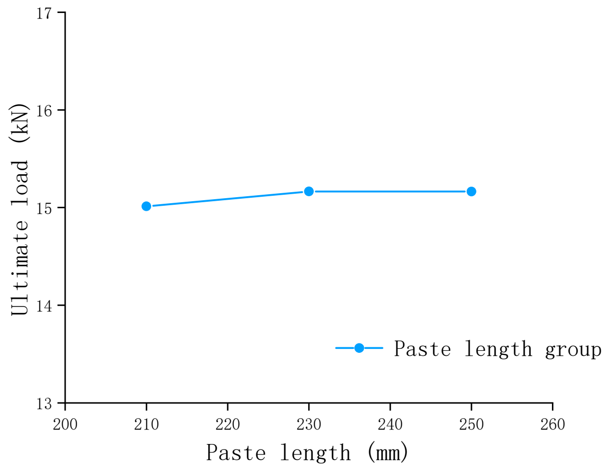

Figure 15. Effect of bond length

The relationship between the ultimate load and the paste length of prestressed CFRP fabric is depicted in Fig. 15. As the paste length of CFRP fabric increases, the specimen's ultimate load capacity essentially remains the same. Related experiments have shown that the CFRP-steel bond contact has an effective bond length [13][29]. The ultimate strength of the CFRP-steel interface increases with the CFRP bond length, similar to the CFRP-concrete interface. Once the bond length reaches a certain value, the ultimate load capacity remains constant. Additionally, there is an effective bond length for the prestressed CFRP-steel interface. The visual analysis from the simulation indicates that the specimens in group E have an effective bond length of approximately 40mm. Moreover, the bond length of the specimens is significantly longer than the effective bond length, suggesting that the bond length of the CFRP fabric has minimal impact on the ultimate load.

5.3. Load-loading end displacement curve

The relationship between the load and the end displacement of the specimen is influenced by the level of prestressing of the CFRP fabric, bond length, number of layers, width, and thickness of the adhesive layer. This section introduces a simplified model of the load-end displacement curve, depicted in Fig. 16. The expression is as follows:

$$\begin{cases} P = ks & 0 < s \le \delta_{\mathrm{f}} \\ P = P_{\mathrm{u}} & s > \delta_{\mathrm{f}} \end{cases} \tag{5}$$

Where k is the slope between the origin (0,0) and the inflection point (δ_f,P_u), which represents the ability of the specimen to resist deformation and reflects the stiffness of the prestressed CFRP-steel interface. Ductility refers to the ability of plastic deformation of the material before

ISSN: 2710-0588

destruction, and in this paper, the ductility of the interface refers to the stage from the load capacity just reaching the ultimate load capacity to the complete destruction of the member, which is the AB section in Fig. 16.

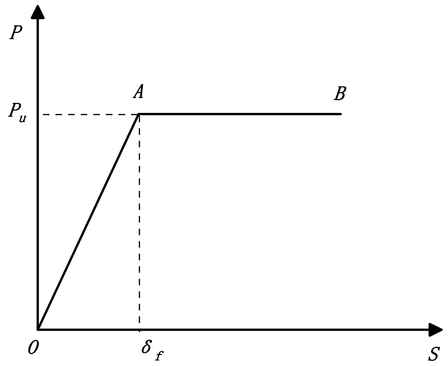

Figure 16. Simplified load-loading end displacement curve model

As can be seen from the figure, the curves of each specimen roughly exhibit a two-stage development pattern: (1) the initial stage OA: at the start of loading, the curves are essentially linear, and the interfacial properties display a better linear shape, capable of withstanding a significant load within a few millimeters of displacement; (2) the plateau stage AB: as the loading increases, damage begins to appear in the adhesive layer unit, leading to a gradual deterioration of the interfacial properties. Despite the adhesive layer not being entirely destroyed, the specimen can still sustain the load, resulting in a slower plateau stage in the curve. During this stage, the damage to the adhesive layer progresses continuously from the center of the span towards both ends, until the adhesive layer is completely damaged, leading to peeling. The interfaces used in the specimens of this simulation are all of the same principal structure, and for this reason, the δ_f of the load-end displacement curves of all specimens are essentially the same. The load-load end displacement curves of each group of specimens are shown in Figs. 17-21.

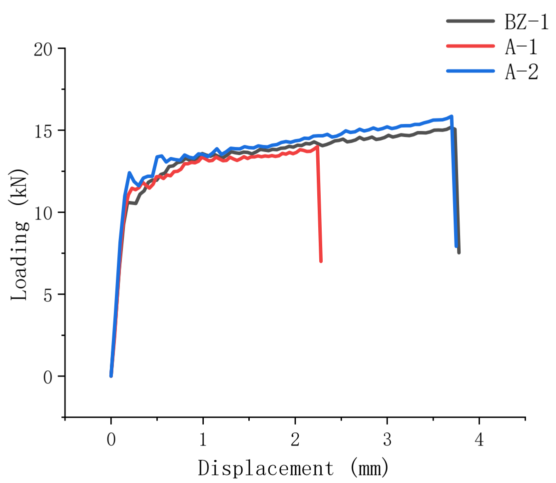

Figure 17. Load-displacement curves at the loading end for the prestressing degree group

The load-displacement curves of the specimens in the various prestressing degree groups don't seem to differ significantly, as seen in Fig. 17. The specimen's ultimate load rises with the prestressing degree; for every 5% increase in the prestressing degree, the specimen's ultimate load can increase by approximately 1kN. The ductility of specimens can be enhanced by raising the prestressing degree of CFRP fabric, as specimen A-1 has the smallest damage displacement within the 5%-15% prestressing degree, measuring only 2.28mm, whereas specimens BZ-1 and A-2 have damage displacements of approximately 3.7mm.

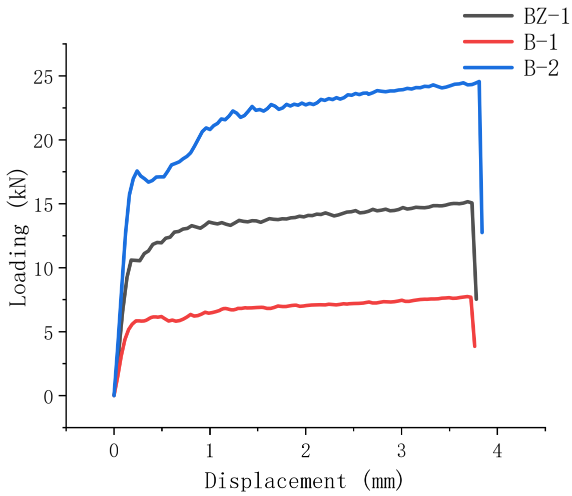

Figure 18. Load-displacement curves at loading end for bond width groups

Figure 18 illustrates how there was a significant variation in the load-displacement curves of the specimens in the various bond width groups. The specimens' ultimate load increased and their rigidity considerably improved as the bond width increased. The stiffness rose from 25.596 to 58.864 and 73.15 when the paste width grew from 20 to 40 and 60 mm, respectively. The average increase in stiffness for every 20 mm increase in width was almost 24%.Although not as much as the reduction in stiffness, the specimens' ductility was also enhanced by the increase in paste width.

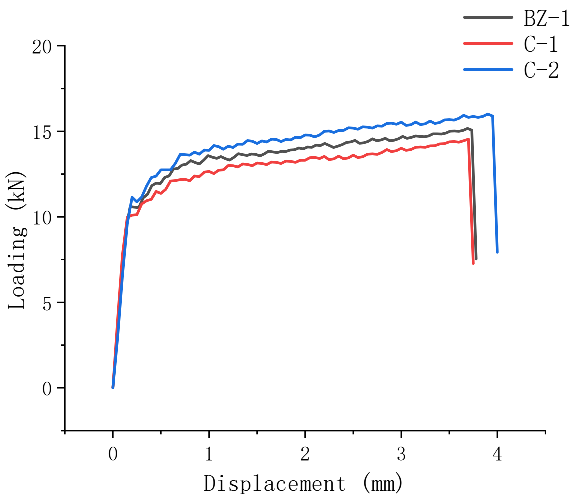

Figure 19. Load-displacement curves at the loading end for the adhesive layer thickness group

ISSN: 2710-0588

The load-displacement curves for the adhesive layer thickness group are displayed in Fig. 19. The figure illustrates how increasing the adhesive layer's thickness within the range of 0.3, 0.5, and 0.7 mm greatly enhances the specimens' ultimate load and ductility. It demonstrates that, with all other factors held constant, 0.7 mm is the ideal choice within the range of adhesive layer thickness from 0.3 to 0.7 mm.

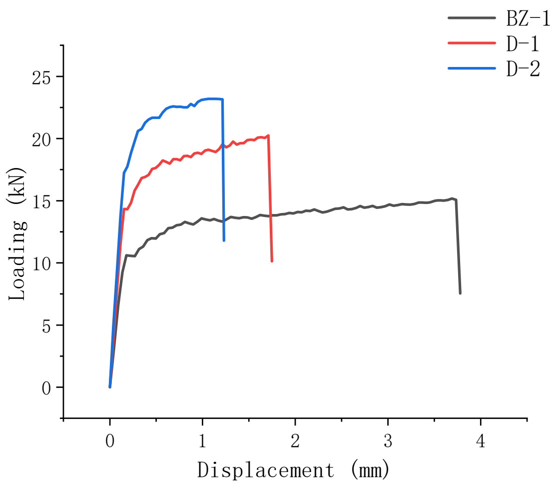

Figure 20. Load-loading end displacement curves for the array of CFRP fabric layers

The load-loading end displacement curves for the number of layers of prestressed CFRP fabric are displayed in Figure 20. The graph illustrates how the interface stiffness and ultimate load capacity of CFRP fabric can be successfully increased by adding more bonded layers. The ultimate load increases by 33.5% and 52.96%, respectively, when 2 and 3 layers are added to a single layer, with an average increase of roughly 25% for a single layer. As the amount of CFRP fabric increases, the damage displacement trends downward. When compared to other variable parameters, the reduction in the specimens' ductility is most clearly caused by the number of layers of prestressed CFRP fabric; damage displacements decrease by 2.025 mm and 2.519 mm, respectively, when the number of layers increases from one to two and three layers.

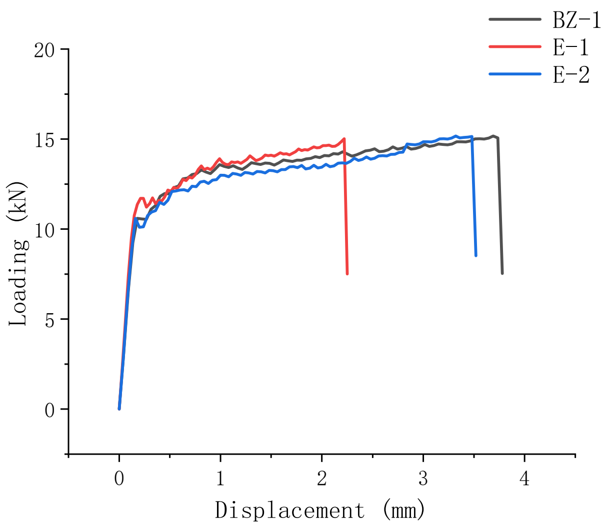

Figure 21. Load-load end displacement curve for bond length group

ISSN: 2710-0588

Fig. 21 illustrates the load-end displacement curves for the bond length group. The interface stiffness, ultimate bearing capacity, and specimen curve shape are all mostly unaffected by the bond length of prestressed CFRP when it exceeds the effective bond length. However, the damage displacement increases as the bond length increases. Specifically, the damage displacement increases by 1.26 mm and 1.515 mm when the bond length is extended from 210 mm to 230 mm and 250 mm, respectively. This indicates that increasing the bond length can improve the specimen's ductility.

5.4. Bond-slip relationship

The interface-slip eigenstructure, also known as the shear stress-slip curve or τ-s curve, allows for the quantitative characterization of the macroscopic load-bearing properties of the interface as well as the local stresses at the interface and the bond failure process. It is assumed in the theoretical study that throughout the elastic phase, the changes at each point are homogeneous and that the stress distribution at the CFRP fabric's cross-section is uniform. Because of this, the pre-stressed CFRP-steel interface bond performance experiment should choose to analyze the bond-slip curve at a typical position as a reference. The bond-slip curve in this test, which underwent a full shear stress fluctuation transfer process, was chosen for reference analysis at a distance of 20 mm from the span center. Each set of specimens' bond-slip curves is displayed in Figures 22–26, and each form displays a double line type.

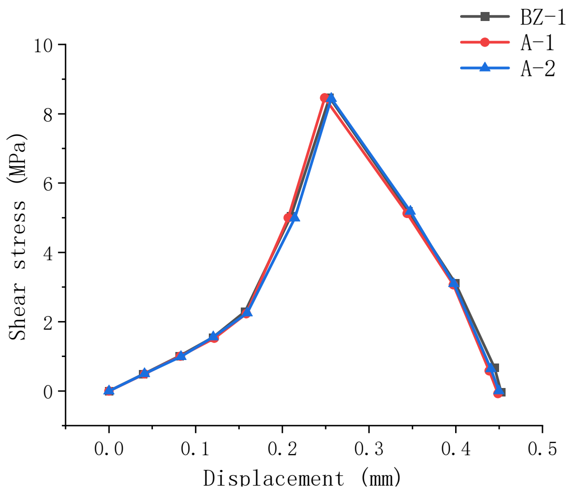

Figure 22. Bond-slip curves for prestressing degree groups

Table 4. Parameters of bond-slip curves for prestressing degree groups

Specimen number	Maximum shear stress τ_0	Slip S_0	Maximum slip S_{MAX}	Interfacial rigidity τ_0/S_0
BZ-1	8.468	0.254	0.452	33.339
A-1	8.46	0.249	0.449	33.976
A-2	8.44	0.256	0.450	32.969

The bond-slip curves for the prestressing degree group are displayed in Figure 22, where the specimen curves nearly overlap. The bond-slip curve parameters for the prestressing degree groups are shown in Table 4, where it is observed that the curve parameters are nearly identical. It is evident from the graphs that the bond-slip curves at the prestressed CFRP-steel interface are essentially unaffected by changes in prestressing degree.

ISSN: 2710-0588

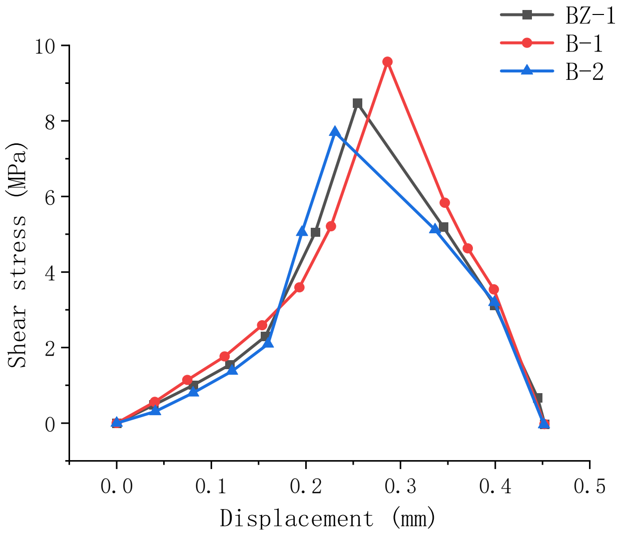

Figure 23. Bond-slip curves for bond width groups

Table 5. Parameters of bond-slip curves for bond width groups

Specimen number	Maximum shear stress τ_0	Slip S_0	Maximum slip S_{MAX}	Interfacial rigidity τ_0 / S_0
B-1	9.563	0.287	0.452	33.321
BZ-1	8.468	0.254	0.452	33.339
B-2	7.700	0.231	0.452	33.335

Fig. 23 illustrates the bond-slip curves for the bond width group. The maximum shear stress at the interface and the corresponding slip both decrease as the bond width increases, while the maximum slip remains relatively constant. The bond-slip curve parameters for the bonding width group are presented in Table 5. It is noted that the interface stiffness of the specimens remained consistent despite changes in bond width. This is because increasing the bond width does not affect the maximum slip but leads to a more uniform distribution of interface shear stress and a reduction in the local maximum shear stress.

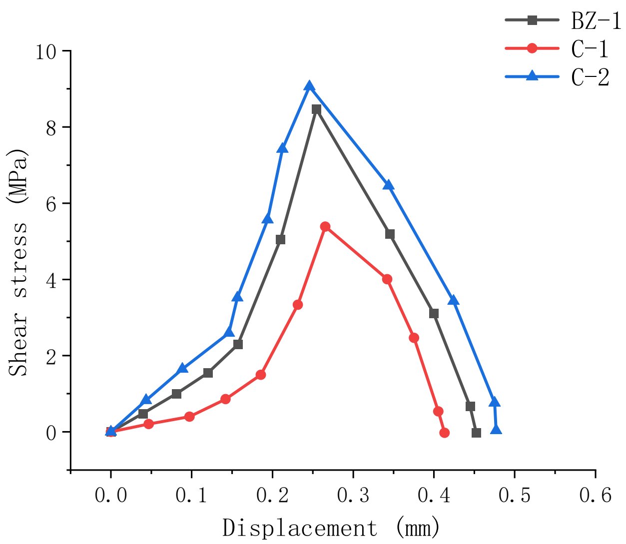

Figure 24. Bond-slip curves for adhesive layer thickness groups

ISSN: 2710-0588

Table 6. Parameters of bond-slip curves for adhesive layer thickness group

Specimen number	Maximum shear stress τ_0	Slip S_0	Maximum slip S_{MAX}	Interfacial rigidity τ_0 / S_0
C-1	5.387	0.265	0.413	20.328
BZ-1	8.468	0.254	0.452	33.339
C-2	9.060	0.246	0.476	36.829

Fig. 24 illustrates the bond-slip curves of the adhesive layer thickness groups. It is observed that the maximum shear stress, slip amount, and maximum slip amount all increase as the adhesive layer thickness increases. The overall bond-slip curve also expands. Table 6 presents the characteristics of the bond-slip curves for the adhesive layer thickness groups. The interfacial stiffness shows a nonlinear relationship as the adhesive layer thickness increases from 0.3 mm to 0.5 mm and 0.7 mm, with increments of 13.001 and 16.501, respectively. With the adhesive layer thickness ranging from 0.3 to 0.7 mm, the greater the thickness of the layer, the better the bonding performance of the interface.

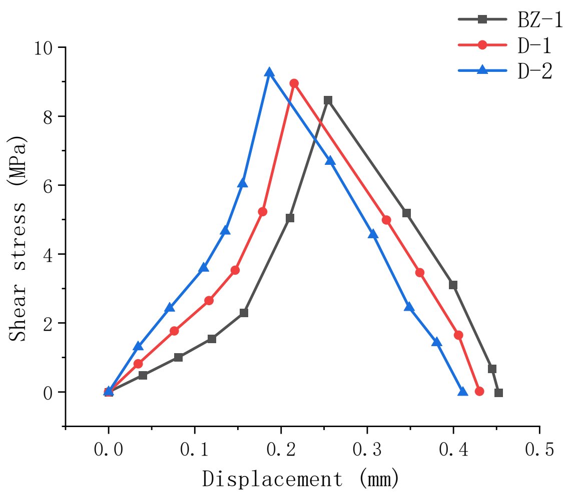

Figure 25. Bond-slip curves for CFRP fabric layer arrays

Table 7. CFRP fabric layer array bond-slip curve parameters

Specimen number	Maximum shear stress τ_0	Slip S_0	Maximum slip S_{MAX}	Interfacial rigidity τ_0 / S_0
BZ-1	8.468	0.254	0.452	33.339
D-1	8.952	0.215	0.430	41.637
D-2	9.252	0.187	0.411	49.476

The bond-slip relationship curves of specimens with varying numbers of prestressed CFRP fabric layers are displayed in Figure 25. The thickness and stiffness of the CFRP fabric increase in proportion to the number of bonded layers in the fabric. The maximum shear stress rises, while the slip and maximum slip tend to decrease as the number of layers of prestressed CFRP fabric grows. In other words, the number of layers of CFRP fabric influences the bond-slip relationship at the specimen interface. The bond-slip relationship parameters of specimens with varying numbers of prestressing CFRP fabric layers are displayed in Table 7. From Table 7, it is concluded that the increase in the number of prestressed CFRP fabric layers resulted in enhancing the specimen interface's ability to resist deformation. The interface stiffness

ISSN: 2710-0588

increased with the increase in the number of CFRP fabric layers, with the interface stiffness increasing by about 24% for every additional layer, showing a linear relationship. However, the maximum slip of the interface decreases with the increase in the number of layers of CFRP fabric, indicating that increasing the number of layers of CFRP fabric reduces the ductility of the members.

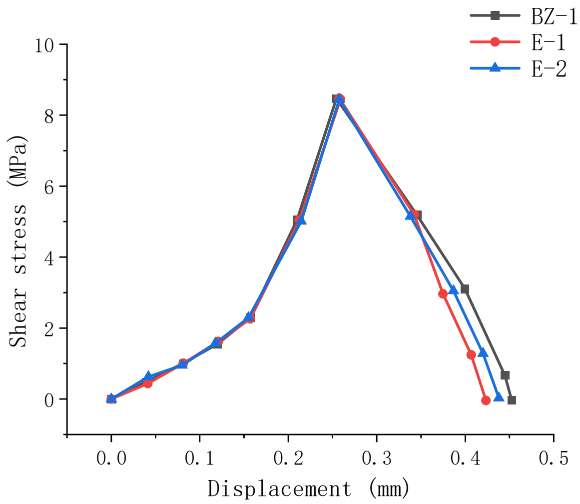

Figure 26. Bond-slip curves for bond length groups

Table 8. Parameters of bond-slip curves for bond length groups

Specimen number	Maximum shear stress τ_0	Slip S_0	Maximum slip S_{MAX}	Interfacial rigidity τ_0 / S_0
E-1	8.491	0.249	0.451	34.100
E-2	8.549	0.258	0.451	33.136
BZ-1	8.468	0.254	0.452	33.339

Fig. 26 displays the bond-slip curves of specimens with various bond lengths. The analysis of the figure shows that the maximum shear stress, slip, and maximum slip are essentially unaffected by an increase in bond length. The bond-slip relationship parameters of specimens from different paste length groups are presented in Table 7. Table 7 indicates that an increase in paste length does not have a discernible impact on the specimen interface's resistance to deformation, nor does it significantly alter the stiffness of the interface. However, the maximum slip of the interface increases with the paste length, suggesting that increasing the paste length can enhance the members' ductility.

6. Conclusion

The prestressed CFRP-steel single-shear specimen model was established using the finite element software ABAQUS. The degree of prestressing of the CFRP cloth, the number of layers, the paste width, the paste length, and the thickness of the adhesive layer were considered as parameters to study the pasting performance of the prestressed CFRP-steel interface. The study led to the following conclusions:

(1) The main damage mode of the prestressed CFRP-steel single shear specimens is cohesive damage in the adhesive layer; at this point, the peak stress of the prestressed CFRP fabric has not reached the limit state.

(2) The presence of prestressing in the specimen offsets part of the external force action, allowing the adhesive layer to bear more shear force. This improves the bonding performance of the interface, contributing to the stability of the specimen.

(3) The load-load end displacement curves of the prestressed CFRP-steel specimens exhibit a two-stage development pattern. The level of prestressing of the CFRP fabric, the width of the paste, and the thickness of the adhesive layer enhance the ultimate load and ductility of the specimens. Conversely, adding more layers of CFRP fabric only boosts the ultimate load, reducing ductility instead.

(4) Changes in the degree of prestressing, width, and length of CFRP fabric do not have a significant effect on the bond-slip relationship of the specimens. The interfacial stiffness remains unchanged. However, increasing the thickness of the adhesive layer within the range of 0.3 mm to 0.7 mm can enhance the interfacial stiffness in a nonlinear manner. Moreover, adding more layers of prestressed CFRP fabric, ranging from 1 to 3, results in a linear increase of 24% in the interfacial stiffness of the specimens per additional layer.

References

[1] Mei, Sunflower, Wang, Fengxuan & Sun, Shengjiang. 2011 A new genus and species of the genus Araneae (Hymenoptera, Braconidae, Araneae) from China. (2024). Progress of fiber-reinforced composites for reinforcing concrete bridge structures. Journal of Building Science and Engineering (01), 31-51. doi:10.19815/j.jace.2022.09044. (in Chinese)

[2] Lu, Yiyan. (2018). Research progress of fiber-reinforced composites and steel composite reinforcement of concrete structures. Journal of Building Structures (10), 138-146. doi:10.14006/j.jzjgxb.2018.10.016. (in Chinese)

[3] Pang, Y., Wu, G., Wang, H., Gao, D., & Zhang, P. (2021). Bond-slip model of the CFRP-steel interface with the CFRP delamination failure. Composite Structures, 256, 113015.

[4] Jingshu Ding, Peng Niu, Xiaochu Wang, Chunfu Jin & Qiang Guo. 2011 A new species of the genus Pterostilbene (Hymenoptera, Braconidae, Pterostilbene). (2020). Research process of prestressed CFRP panels for reinforcing concrete bridges. Concrete (09), 133-138. (in Chinese)

[5] Wang, X. L., Li, Chaofeng & Li, Ke. (2019). Experimental analysis of bond performance of damaged reinforced concrete beams reinforced with CFRP fabric under fatigue loading. Building Structures (03), 87-91. doi:10.19701/j.jzjg.2019.03.016. (in Chinese)

[6] Lü, Z., Xu, H. B. & Yu, C. C... (2022). A review of CFRP-steel bond performance under fatigue loading. Structural Engineer (05), 177-181. doi:10.15935/j.cnki.jggcs.2022.05.011. (in Chinese)

[7] Zhang, L.. (2020). Experimental and theoretical analysis of bonding performance of CFRP-steel interface under static and fatigue loading Ph.D. (Dissertation, Southeast University). Ph.D. https://link.cnki.net/doi/10.27014/d.cnki.gdnau.2020.000066doi:10.27014/d.cnki.gdnau.2020.000066. (in Chinese)

[8] Teng, J. G., Yu, T., & Fernando, D. (2012). Strengthening of steel structures with fiber-reinforced polymer composites. Journal of constructional steel research, 78, 131-143.

[9] Chuanxi Li, Lu Ke, Zhuoyi Chen, Jun He & Nanhai Luo. (2018).Experimental and numerical simulation of bonding performance of CFRP-steel interface. Journal of Composite Materials (12), 3534-3546. doi:10.13801/j.cnki.fhclxb.20180316.001. (in Chinese)

[10] Hu, Lili. (2020). Study on the Overall Stability of Steel Columns Reinforced by Prestressed Carbon Fiber Composite Plates Ph.D. (Dissertation, Tsinghua University). Ph.D. https://link.cnki.net/doi/10.27266/d.cnki.gqhau.2020.000045doi:10.27266/d.cnki.gqhau.2020.000045. (in Chinese)

[11] Wong, K. F.. (2020). Master of Science (Dissertation, South China University of Technology) on bonding performance of CFRP-steel plate interface under static loading. Master https://link.cnki.net/doi/10.27151/d.cnki.ghnlu.2020.002514doi:10.27151/d.cnki.ghnlu.2020.002514. (in Chinese)

[12] Zhao, X. L., & Zhang, L. (2007). State-of-the-art review on FRP strengthened steel structures. Engineering structures, 29(8), 1808-1823.

[13] Lu, Yi-Yan, Zhang, No. J. & Liu, S. L. (2006). (2006). Study on the shear properties of carbon fiber cloth bonded to steel plates. Journal of Civil Engineering (10), 60-67. (in Chinese)

[14] Triantafillou, T. C., & Deskovic, N. (1991). Innovative prestressing with FRP sheets: mechanics of short-term behavior. Journal of Engineering Mechanics, 117(7), 1652-1672.

[15] Yeh, Hwa-Wen. (2009). Experimental Study on Tensile Static and Fatigue Performance of Prestressed Carbon Fiber Plate (CFRP) Reinforced Steel Plates Ph.D. (Dissertation, Southwest Jiaotong University). Ph.D. https://kns.cnki.net/kcms2/article/abstract?v=WYPw_9jmhsI0YhlYWtwTPPTsRxpUBsPSLmggzQr_UtJDdyw0ewsh4jKQv31diTzSvWC-JMkCMdCnLCg4lKqVPfCSx-lpT_OPMsnOek_0JAPk9O7d7ETFL00c03e-k33pRfawel0yIxe5V-sO7hlMbiJaYN7UnvvnTsabppnaEMnGyH4AzwD7EIyTWmasXy75&uniplatform=NZKPT&language=CHS (in Chinese)

[16] Guangshan Zhu, Fusheng Zhu, Guohua Sheng & Zuoxin Ma. (2018). Flexural load, stiffness and crack analysis of prestressed CFRP and steel plate reinforced T-beams. Journal of Shenyang University of Architecture(Natural Science Edition)(02),211-221. (in Chinese)

[17] Guangshan Zhu, Fusheng Zhu & Guohua Sheng. (2018). Flexural performance test of pre-stressed CFRP and steel plate composite reinforced T-beam. Journal of Northeastern University (Natural Science Edition)(04),594-598. (in Chinese)

[18] Wu Hao, Lu Si-Yu & Chen D. A study on the dynamic shear behavior of FRP-concrete bond interface based on 3D fine-scale modeling. Study on dynamic shear behavior of FRP-concrete bond interface based on 3D fine view model of concrete. Engineering Mechanics 1-16. (in Chinese)

[19] Lu, X. Z., Ye, L. P., Teng, J. G., & Jiang, J. J. (2005). Meso-scale finite element model for FRP sheets/plates bonded to concrete. Engineering structures, 27(4), 564-575.

[20] He, Suo-Jie, Xu, Tao, Song, Baodong & Tang, Chunan. (2012).Numerical simulation study on the effect of FRP plate width on the interfacial bond performance of concrete. Building Structures (S1), 794-800. doi:10.19701/j.jzjg.2012.s1.196. (in Chinese)

[21] Yang, Y., Huang, K. F. & Wu, C. D.. (2021). Study on the bonding performance of CFRP-steel plate interface based on double shear experiment. Journal of Sun Yat-sen University (Natural Science Edition) (06), 62-70. doi:10.13471/j.cnki.acta.snus.2020.07.14.2020b082. (in Chinese)

[22] LI Teng, NING Zhihua, WU Jiayu. Experimental study and numerical simulation of bonding performance of CFRP reinforced steel plates in marine environment[J]. Materials Engineering, 2022: 1-15. (in Chinese)

[23] Cynthia Yu, Yizhou Zhao & Ruixin Gao. (2022). Influence of marine atmospheric environment on the bonding performance of CFRP-steel interface. Journal of Composite Materials (11), 5148-5157. doi:10.13801/j.cnki.fhclxb.20220915.003. (in Chinese)

[24] He J. (2017). Study on the effect of adhesive properties on bond damage behavior of CFRP-steel interface Ph.D. (Dissertation, Harbin Institute of Technology). Ph.D. https://kns.cnki.net/kcms2/article/abstract?v=WYPw_9jmhsKnUDKllyIUE-9tcGuMoSzKlNtHtZZh3us_HX_yEyboDFdRshk8UBwXq9sfkOY1WuxRilSfPLt6xaFtQ1Vf0zBFPzjvmYCI9q5jFMIDbqCnzZXMG4v4vDM88n0q02lJykwgPN28GA1fplZ8dRwNPlVv8xDKYzjJJSd-B8v6H6Xo4XmUcpnecX1Zt0HnlxS5tyg=&uniplatform=NZKPT&language=CHS (in Chinese)

[25] Wu Zuodong. (2022).M.S. (Dissertation, South China University of Technology) on bond-slip relationship of bonded layers of CFRP reinforced steel plates. M.S.https://link.cnki.net/doi/10.27151/d.cnki.ghnlu.2022.005632doi:10.27151/d.cnki.ghnlu.2022.005632.(in Chinese)

[26] Xia, S. H., & Teng, J. (2005, January). Behaviour of FRP-to-steel bonded joints. In International Symposium on Bond Behaviour of FRP in Structures, BBFS 2005 (pp. 411-418). International Institute for FRP in Construction (IIFC).

ISSN: 2710-0588

[27] Director Er, Mangliang Ma & Yiheng Wang. (2019). Strengthening coefficients and parametric analysis of prestressed CFRP plate bonded H-beams. FRP/Composites (04), 17-24. (in Chinese)

[28] Wang, K. J.. (2020). Numerical analysis of prestressed FRP-reinforced concrete flexural members M.S. (Dissertation, Dalian University of Technology). Master https://link.cnki.net/doi/10.26991/d.cnki.gdllu.2020.000428doi:10.26991/d.cnki.gdllu.2020.000428. (in Chinese)

[29] Liu, S. L.. (2004). Study on the bonding mechanism between carbon fibre cloth and steel plate M.S. (Dissertation, Wuhan University). M.S. (Dissertation, Wuhan University). https://kns.cnki.net/kcms2/article/abstract?v=sgrnXhMyarYVSU3qEjwIHgmUI2fKjipEYtI_ZKbJ9p4KciV2lmpNRn3P-B5HrGPPeWHiab-4zc8dM8IhjfL0ctONpMXvQs6iCvQfZzferyPlHS95GhyYQDzO4Tr7GQemFOiawCc7kmXM3XCVVg-v-MBKaDy7oKpvo2XIZx0gGSqGvYtC7QVnEFC8Dor2seis&uniplatform=NZKPT&language=CHS. (in Chinese)